DOI: 10.48011/sbse.v1i1.2496

Eight Thyristor AC-DC Modified Converter Bridge Implementation

Marcos Leonardo Ramos*. José Maria de Carvalho Filho. Ângelo José Junqueira Rezek***. Christel Enock Ghislain Ogoulola****. Vinicius Zimmermann Silva*****

**Federal University of Itajubá, ISEE-UNIFEI*
Itajubá, MG, Brazil, (marcoslramos@hotmail.com)
***Federal University of Itajubá, ISEE-UNIFEI*
Itajubá, MG, Brazil, (jmaria@unifei.edu.br)
****Federal University of Itajubá, ISEE-UNIFEI*
Itajubá, MG, Brazil, (rezek@unifei.edu.br)
*****Federal University of Itajubá, ISEE-UNIFEI*
Itajubá, MG, Brazil, (christel@unifei.edu.br)
******Federal University of Itajubá, ISEE-UNIFEI*
Itajubá, MG, Brazil, (vinicius.zimmermann@yahoo.com.br)

Abstract: The purpose of this work is to implement at laboratory a full-controlled AC-DC test bench operating as a modified bridge and a conventional bridge, considering for both bridge the same average DC output voltage criterion. Furthermore, the performance of the test bench can be verified by checking the consistency of the experimental results between the modified bridge and the conventional bridge, as well as the consistency of the experimental results of these bridges with their theoretical values and digital simulations. It is expected the test bench can be applied for didactic and research purposes as well as for industrial applications.

Keywords: auxiliary firing; modified converter; modified thyristor bridge; improved power factor; modified phase-controlled converter.

1. INTRODUCTION

The purpose of this study is to test at laboratory a modified AC-DC bridge. The motivation behind this study is based on theoretical concepts and comparative analysis of the power factor performance between modified six-pulse phase-commutated converter and conventional six-pulse phase-commutated converter, as presented in V.R. Stefanovic 1979. Studies on AC-DC converters for applications in electrical power plants are of great importance given the implications for improving power factors and avoiding additional costs in electric energy bills. As a contribution, this study can be applied for didactic and research purposes as well as for industrial purposes.

The modified AC-DC bridge was implemented at the Federal University of Itajubá (UNIFEI) laboratory for a test bench, and was equipped with digital meter (see Fig. 1 and Fig. 2). The test bench worked under two operation modes considering the same average DC output voltage criterion, so that in mode 1 it worked as a modified bridge, and in mode 2 it worked as a conventional bridge.

The modified bridge is a six-pulse AC-DC converter bridge and operates as a full-controlled rectifier in a Graetz configuration, powered by a 4-wire three-phase electrical system, equipped with eight thyristors and two independent firing control circuits. The conventional bridge was set in a particular operational mode of the modified bridge so that when auxiliary firing is de-energized, the modified bridge operates as a conventional bridge (A.J.J. Rezek 1990, G. Oliver 1980 and V.R. Stefanovic 1979).

Theoretical concepts like modified bridge operation for different firing angles of the phase thyristors and neutral thyristors (A.J.J. Rezek 1990) and V.R. Stefanovic 1979), digital simulations for current and voltage waveforms (A.J.J. Rezek 1990), and modified and conventional bridge equations (A.J.J. Rezek (1990), G. Oliver (1980), V.R. Stefanovic (1979), J.A. Pomílio (2019), J.M. Schaefer (1965)), are all discussed in Section 2.

Both the six-pulse thyristor firing electronic board operation, and the topologies of the main and the auxiliary firing control circuits of the modified bridge based on the electronic board (G. Oliver 1 (980), G.R.S. Mendonça (2002), M.C. Cardoso (2016/2017) and M.L. Ramos (2017)), are discussed in Section 3.

The recorded experimental test data obtained for the voltage waveforms, the current waveforms, and the electrical measurements for the modified and conventional bridges are presented in Section 4.

The experimental test analysis of Section 4, considering the consistency of the experimental results between the bridges, the consistency of the experimental results of the bridges with their theoretical concepts and digital simulations, and the voltage and current waveforms plotted on Matlab/Simulink, are all discussed in Section 5.

The final conclusions are presented in Section 6.

The electrical diagram of the test bench is shown in Fig. 1, where: **A** is the ammeter; **AFCC** is the auxiliary firing control circuit of the neutral thyristors; **G1, G2, G3, G4, G5,**

G6, G7, G8 are the thyristor gates; **Io** is the average DC output current; **Ia, Ib, Ic** are the AC input current; **I_N** is the AC neutral current; **K1, K2, K3, K4, K5, K6, K7, K8** are the thyristor cathodes; **L** is the inductance; **MFCC** is the main firing control circuit of the phase thyristors; **NTHY** are the neutral thyristors; **PQA** is the power quality analyzer; **PTHY** are the phase thyristors; **R** is the resistance; **SCP-1, SCP-2** are the oscilloscopes; **SSM** is the signal splitter module; **T1, T2, T3, T4, T5, T6, T7, T8** are the thyristors; **V** is the voltmeter; **Vo** is the average DC output voltage; **VNn** is the pole N voltage with respect to the power source neutral; **VPn** is the pole P voltage with respect to the power source neutral; **VPN** is the DC output voltage.

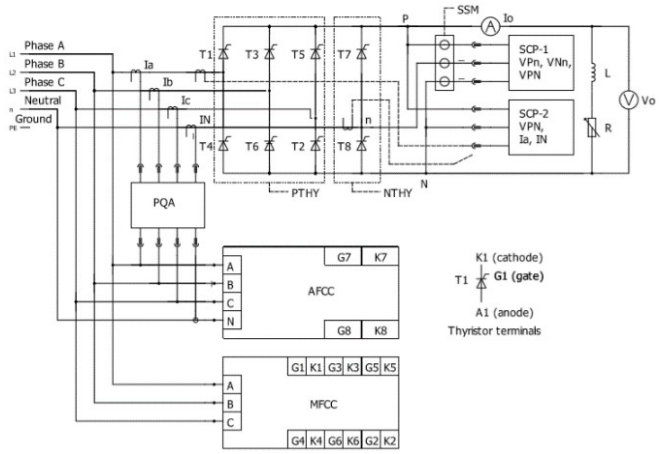

Fig. 1: Electrical diagram of the test bench

The test bench is shown in Fig. 2, where DM1 and DM2 are the diode modules.

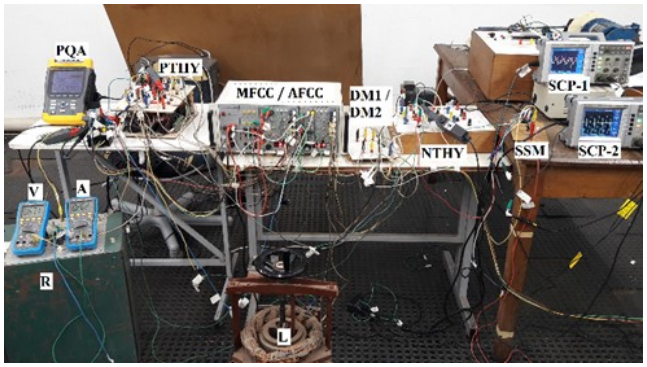

Fig. 2: Test bench

2. THEORETICAL CONCEPTS

2.1 General

According to A.J.J. Rezek 1990) and V.R. Stefanovic 1979, the DC output voltage of the modified bridge depends on the sets of the main angle (α) and the auxiliary angle (δ), as follow:

a) For $0^0 \leq \alpha \leq 30^0$ and $\delta \geq 0^0$: the modified bridge works the same way as the conventional bridge; the phase thyristors of the modified bridge work, and the neutral thyristors do not work; the DC output voltage of the modified bridge is composed only by phase-to-phase of the AC input voltage of the modified bridge; the neutral thyristors are ineffective if $0^0 \leq \alpha \leq 30^0$ and $\delta \geq 0^0$ (see Fig. 3).

b) For $30^0 < \alpha \leq 150^0$ and $\delta \geq 0^0$: the modified bridge works differently the conventional bridge; the phase thyristors and the neutral thyristors work; the DC output voltage of the modified bridge is composed of a phase-to-phase AC input voltage and a phase-to-neutral AC input voltage for the modified bridge (see Fig. 4).

According to V.R. Stefanovic 1979, there are advantages to using a modified bridge over a conventional bridge when considering the same average DC output voltage criterion. These advantages may be DC: harmonic content; lower requirements for reactive power, especially at reduced DC voltage; lower rms current at reduced power output; and a higher power factor. However, there are disadvantages, which usually include: increased AC harmonic distortion, additional costs due the neutral thyristors and auxiliary firing.

Based on A.J.J. Rezek (1990) it was plotted the current and voltage waveforms of the modified bridge in Matlab/Simulink considering intervals $0^0 \leq \alpha \leq 30^0$ and $\delta \geq 0^0$. It is emphasized that, for the previous intervals, the modified bridge waveforms are equal to the voltage and current waveforms in the conventional bridge with $\alpha \geq 0^0$.

The waveforms are shown in Fig. 3 where: **Ia** is the AC input current of phase A; **I_N** is the AC input current of neutral; **Van** is the phase-to-neutral AC input voltage; **Vab, Vca** are the phase-to-phase AC input voltages; **VNn** is the pole N voltage with respect to the power source neutral; **VPn** is the pole P voltage with respect to the power source neutral; **VPN** is the DC output voltage; **α** is the main angle; and **δ** is the auxiliary angle.

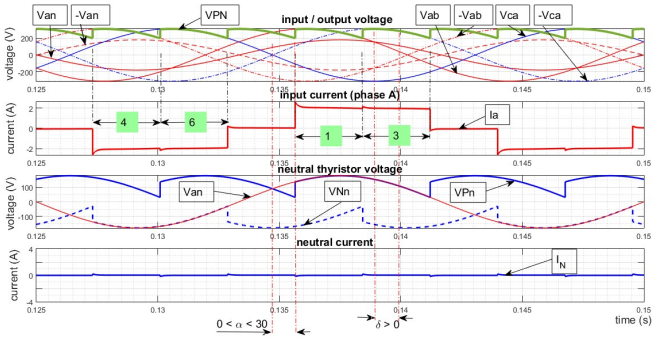

Fig. 3: Modified bridge – voltage and current ($0^0 \leq \alpha \leq 30^0$ and $\delta \geq 0^0$)

The DC output voltage intervals of the modified bridge for the positive and negative half-cycle current of phase A were recorded and are shown in Table 1 (see Fig. 3).

Table 1: Modified bridge – output voltage vs. input current ($0^0 \leq \alpha \leq 30^0$ and $\delta \geq 0^0$)

Current	Half-cycle		Fired thyristor	Interval	Reference
	Positive	Negative			
Ia	V_{ab}		T1-T6	1	Fig.3
	V_{ac}		T1-T2	3	
		$-V_{ab}$	T4-T3	4	
		$-V_{ac}$	T4-T5	6	

In the Fig. 4 ($30^0 < \alpha \leq 150^0$ and $\delta \geq 0^0$), the voltages, currents and settings angles for the modified bridge are shown.

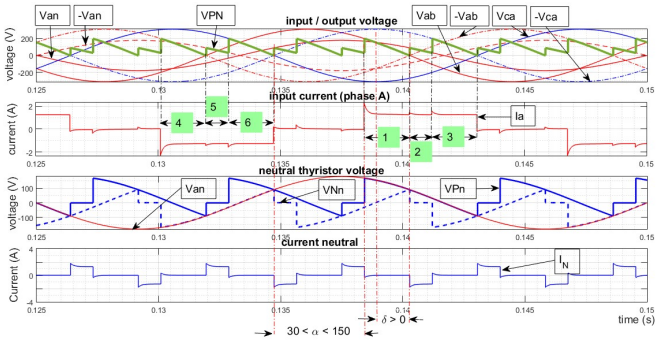

Fig. 4: Modified bridge – voltage and current ($30^0 < \alpha \leq 150^0$ and $\delta \geq 0^0$)

The DC output voltage intervals of the modified bridge for the positive and negative half-cycle current of phase A were recorded and are shown in Table 2 (see Fig. 4).

Table 2: Modified bridge – output voltage vs. input current ($30^0 < \alpha \leq 150^0$ and $\delta \geq 0^0$)

Current	Half-cycle		Fired thyristor	Interval	Reference
	Positive	Negative			
Ia	V_{ab}		T1-T6	1	Fig.4
	V_{an}		T1-T8	2	
	V_{ac}		T1-T2	3	
		$-V_{ab}$	T4-T3	4	
		$-V_{an}$	T4-T7	5	
		$-V_{ac}$	T4-T5	6	

2.2 Equations applied in modified and conventional bridges

The equations ahead can be applied for test bench that operate with a modified bridge and a conventional bridge. According to A.J.J. Rezek (1990), G. Oliver (1980) and V.R. Stefanovic (1979), if the test bench operates as a modified bridge in the interval $0^0 \leq \alpha \leq 30^0$ and $\delta \geq 0^0$, these equations are to be applied. According to J.A. Pomílio (2019) and J.M. Schaefer (1965), if the test bench operates as a conventional bridge with $\alpha \geq 0^0$, these equations are applied too. The equations are:

a) Average output voltage:

$$V_0 = [(3\sqrt{2}) / \pi] \, . \, V_{RMS} \, . \cos(\alpha) \quad (1)$$

where: **Vo** is the average DC output voltage; $\mathbf{V_{RMS}}$ is the rms phase-to-phase AC input voltage; and **α** is the main angle.

b) Displacement factor:

$$DF = \cos(\varphi_1) \quad (2)$$

Where: **DF** is the displacement factor; and $\boldsymbol{\varphi_1}$ (displacement angle) is the angle between rms input fundamental voltage and rms input fundamental current.

c) Distortion factor:

$$D_f = I_1 / I_{RMS} = 3 / \pi \quad (3)$$

Where: $\mathbf{D_f}$ is the distortion factor; $\mathbf{I_1}$ is the rms value of the fundamental AC input current; and $\mathbf{I_{RMS}}$ is the rms value of the total AC input current.

d) Power factor:

$$PF = \cos(\varphi) = D_f \, . \cos(\varphi_1) \quad (4)$$

$$PF = DF / [\sqrt{(1 + (THD)^2)}] \quad (5)$$

$$FP = (3 / \pi) \, . \cos(\propto) \quad (6)$$

Where: **PF** is the power factor; **φ** is the angle between rms total input voltage and rms total input current; $\boldsymbol{\varphi_1}$ (displacement angle) is the angle between rms input fundamental voltage and rms input fundamental current; and **α** is the main angle.

e) Total harmonic distortion:

$$THD = \frac{\sqrt{\sum_{n=2}^{\infty}(I_n)^2}}{I_1} \quad (7)$$

Where: **THD** is the total harmonic distortion; $\mathbf{I_1}$ is the rms value of the fundamental AC input current; **In** is the rms value of the n order AC input current; **n** is the harmonic order.

2.3 Equations applied in modified bridge

According to A.J.J. Rezek (1990), G. Oliver (1980) and V.R. Stefanovic (1979), the test bench operates only as modified bridge in the interval $30^0 < \alpha \leq 150^0$ and $\delta \geq 0^0$, the following equations are applied:

a) Output average voltage:

$$Vo = [(\sqrt{6}) / \pi)] \, . \, V_{RMS} \, . \, [\cos(\alpha + 30^0) + \cos(\delta)] \quad (8)$$

Where: **Vo** is the average DC output voltage; $\mathbf{V_{RMS}}$ is the rms phase-to-phase AC input voltage; **α** is the main angle; and **δ** is the auxiliary angle.

b) Displacement factor:

$$DF = \cos(\varphi_1) = \cos[(\alpha + \delta + 30^0) / 2] \quad (9)$$

Where: **DF** is the displacement factor; $\boldsymbol{\varphi_1}$ is the displacement angle, angle between rms input fundamental voltage and rms input fundamental current; **α** is the main angle; and **δ** is the auxiliary angle.

c) Distortion factor:

$$D_f = I_1 / I_{RMS} \quad (10)$$

Where: $\mathbf{D_f}$ is the distortion factor; $\mathbf{I_1}$ is the rms value of the fundamental AC input current; and $\mathbf{I_{RMS}}$ is the rms value of the total AC input current.

d) Power factor:

$$PF = \cos(\varphi) = D_f \, . \cos(\varphi_1) \quad (11)$$

$$PF = DF / \sqrt{(1 + (THD)^2)} \quad (12)$$

$$PF = (\sqrt{2}) \, . \, [\cos(\propto + \pi/6) + \cos(\delta)] / \{\pi \, . \, [(5/6 + ((\delta - \alpha) / \pi))]^{0,5}\} \quad (13)$$

Where: **PF** is the power factor; **φ** is the angle between rms input voltage and rms total input current; **φ1** (displacement angle) is the angle between rms input fundamental voltage and rms input fundamental current; **α** is the main angle; and **δ** is the auxiliary angle.

Note: **α** and **δ** in equation (13) is given in radian.

e) Total harmonic distortion:

$$\mathbf{THD} = \frac{\sqrt{\sum_{n=2}^{\infty}(I_n)^2}}{I_1} \qquad (14)$$

Where: **THD** is the total harmonic distortion; $\mathbf{I_1}$ is the rms value of the fundamental AC input current; and **In** is the rms value of the AC harmonic input current, order n.

3. MODIFIED BRIDGE FIRING CONTROL CIRCUITS

The firing control circuits topologies for the modified bridge based on six-pulse thyristor firing electronic board, will be described in this section as per G.R.S. Mendonça (2002), M.C. Cardoso (2016/2017) and M.L. Ramos (2017).

3.1 The six-pulse thyristor firing electronic board

The block diagram of the six-pulse thyristor firing electronic board is shown in Fig. 5 with three upper lanes for firing the upper thyristors (T1, T3, T5), and three lower lanes for firing the lower thyristors (T4, T6, T2).

The electronic board also has four stages (1, 2, 3, 4) and four output signals (V1, V2, V3, V4). Stage 1 controls the thyristor firing angle from 0^0 to 180^0 from an independent DC source (+ V_{DC}) and an AC synchronous voltage relative to the thyristor power circuit to be fired. Stage 2 provides the pulse width. Stage 3 transmits the pulse to the next stage and provides electrical isolation between the high and low power circuits. Stage 4 is the attack stage, and consists of current source characteristics for firing thyristors and the negative voltage blockage to the thyristors gate-cathode.

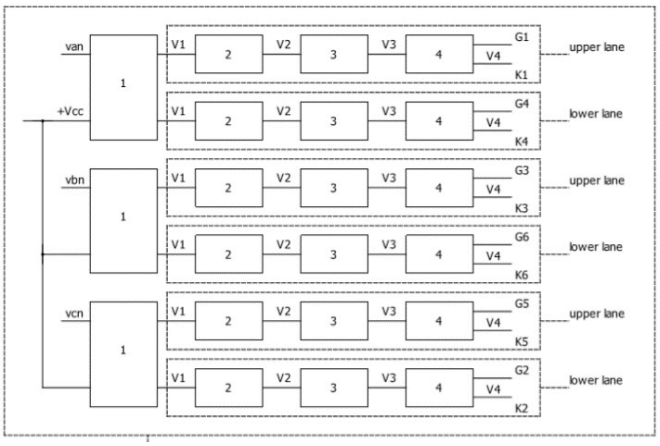

Fig. 5: Block diagram – six-pulse thyristor firing electronic board

3.2 Main firing control circuit

A block diagram of the main firing control circuit (MFCC) is shown in Fig. 6. It was assembled for firing phase thyristors at an angle α setting. The MFCC has one-winding transformers in Δ-Yn configuration (TR-1, TR-2, TR-3), a DC source (RET), and a six-pulse thyristor firing electronic board.

The phase thyristors firing at angle α is set in the interval $0^0 \leq \alpha \leq 150^0$ according to G. Oliver (1980), and should be slightly less than 150^0 due to the commutation interval.

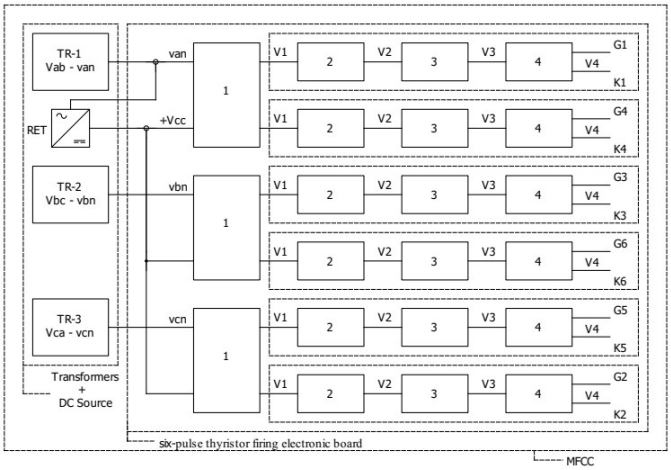

Fig. 6: Block diagram – main firing control circuit

3.3 Auxiliary firing control circuit

A block diagram for the AFCC (auxiliary firing control circuit)is shown in Fig. 7. It was assembled to fire the neutral thyristors at an angle δ setting. The AFCC is composed of one-winding transformers in Yn-Yn configuration (TR-1, TR-2, TR-3), a DC source (RET), two diodes module (DM-1, DM-2) and a six-pulse thyristor firing electronic board.

The neutral thyristors firing angle δ is set in the interval $0^0 \leq \alpha \leq 120^0$ according to G. Oliver (1980), and should be slightly less than 120^0 due to the commutation interval.

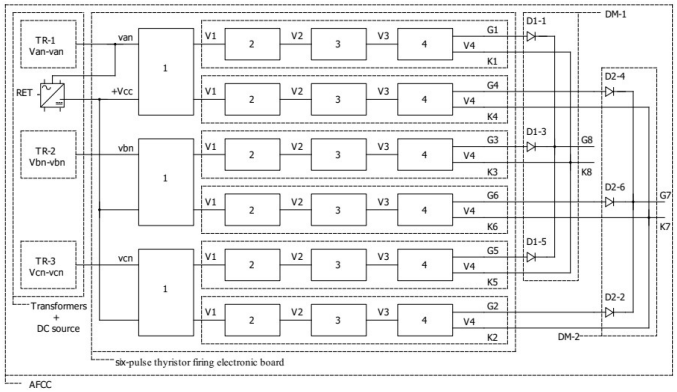

Fig. 7: Block diagram – auxiliary firing control circuit

4. STUDY OF CASE

4.1 General

The test bench was powered by an AC three-phase four wire electrical system, 220V/127V, 60Hz, with a fixed RL load (R = 137Ω, L = 189.4mH). Several tests were conducted for the test bench working as both a modified and conventional bridge with same average DC output voltage. It was studied the power factor, the displacement factor, the total current harmonic distortion, the output voltage waveforms, and the phase and neutral input current waveforms. The test results were compared to the experimental results under different operational modes, and to the experimental and theoretical results.

4.2 Output voltage waveform for $0^0 \leq \alpha \leq 30^0$ and $\delta \geq 0^0$

Bench tests were conducted with a modified bridge at $0^0 \leq \alpha \leq 30^0$ and $\delta \geq 0^0$ and the DC output voltage waveform changed only with angle α and was unchanged when varying angle δ. Thus the modified bridge worked the same way as a conventional bridge.

The auxiliary firing was de-energized, so the test bench worked as a conventional bridge with $0^0 \leq \alpha \leq 30^0$. The previous tests were repeated, and the results were the same as the test bench working as a modified bridge with $0^0 \leq \alpha \leq 30^0$ and $\delta \geq 0^0$.

The waveforms are shown in Fig. 8, for two settings: Vo = 297.10V, $\alpha = 0^0$, $\delta = 0^0$; and Vo = 297.10V, $\alpha = 0^0$, $\delta = 30^0$.

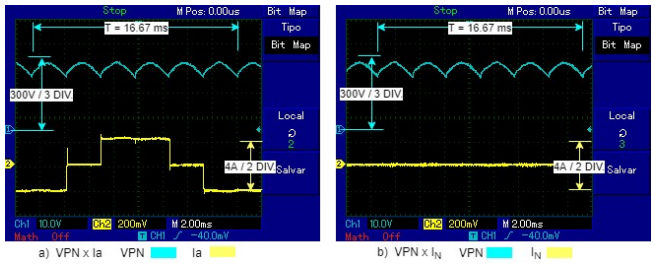

Fig. 8: Modified bridge – output voltage vs. input current

The waveforms shown in Fig. 9 have two settings for the modified bridge (Vo = 297.10V, $\alpha = 0^0$, $\delta = 0^0$ and Vo = 297.10V, $\alpha = 0^0$, $\delta = 30^0$) and one setting for conventional bridge (Vo = 297.10V, $\alpha = 0^0$).

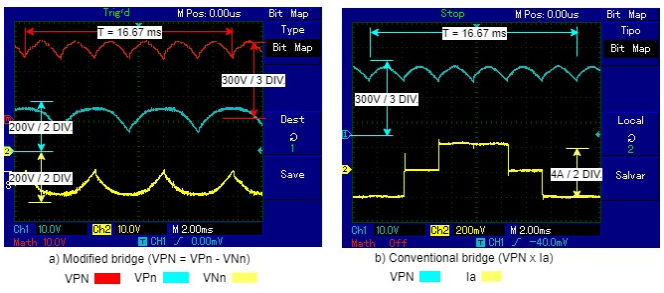

Fig. 9: VPN waveforms for the same average DC output voltage

4.3 Output voltage waveform for $30^0 < \alpha \leq 150^0$ and $\delta \geq 0^0$

A bench test was conducted working as a modified bridge with $30^0 < \alpha \leq 150^0$ and $\delta \geq 0^0$ and the DC output voltage waveform changed when varying angle α or δ. Thus, the modified bridge worked differently from a conventional bridge.

The auxiliary firing was de-energized, so the test bench worked as a conventional bridge with $30^0 < \alpha \leq 150^0$. The previous tests were repeated and the results were different from the bench test working as a modified bridge with $30^0 < \alpha \leq 150^0$ and $\delta \geq 0^0$.

The conventional bridge main angle (α) was set until its average DC output voltage reached the same value as the modified bridge. The main angle of the conventional bridge can be obtained by reading the main angle in the display of the main firing control circuit. It can also be taken by comparing the modified and conventional average DC output voltage equations (equation (1) = equation (8)).

The modified bridge waveforms are shown in Fig. 10, with setting: Vo = 171.53V, $\alpha = 60^0$, $\delta = 0^0$.

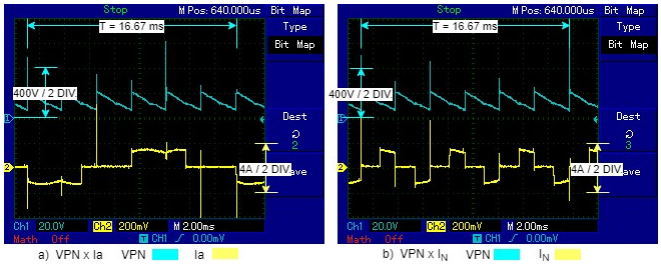

Fig. 10: Modified bridge – output voltage vs. input current

The waveforms are shown in Fig. 11, considering: one setting for a modified bridge, with Vo = 171.53V, $\alpha = 60^0$, $\delta = 0^0$; and one setting for conventional bridge with Vo = 171.53V, $\alpha = 47.10^0$ calculated by comparing the equations.

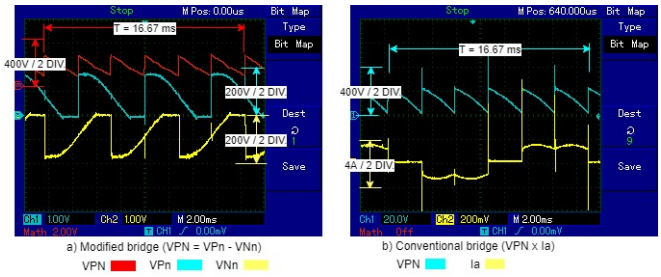

Fig. 11: VPN waveforms for the same average DC output voltage

The modified bridge waveforms are shown in Fig. 12, considering settings Vo = 148.55V, $\alpha = 60^0$, $\delta = 30^0$.

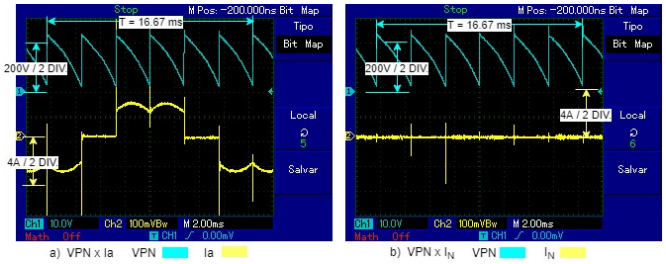

Fig. 12: Modified bridge – output voltage vs. input current

The waveforms for one setting for a modified bridge with Vo = 148.55V, $\alpha = 60^0$, $\delta = 30^0$ and one setting for conventional bridge with Vo = 148.55V, $\alpha = 51.84^0$ calculated by comparison equations, are shown in Fig. 13.

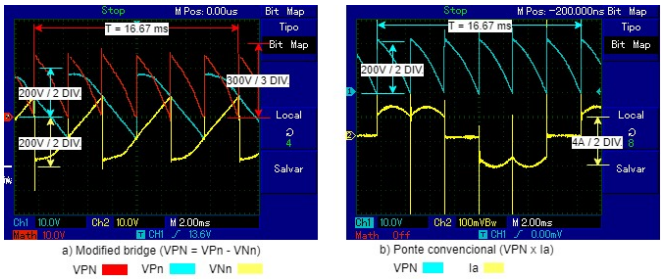

Fig. 13: VPN waveforms for the same average DC output voltage

The modified bridge waveforms for setting Vo = 141.75V, $\alpha = 70^0$, $\delta = 0^0$, are shown in Fig. 14.

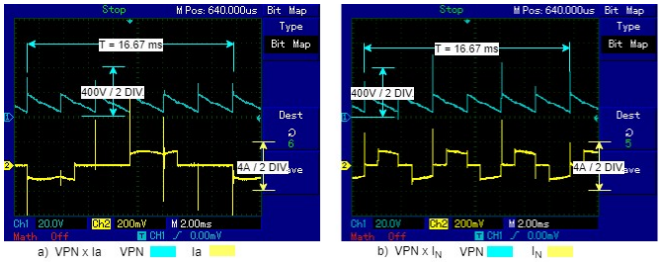

Fig. 14: Modified bridge – output voltage vs. input current

The waveforms for one setting for modified bridge with Vo = 141.75V, $\alpha = 70^0$, $\delta = 0^0$ and one setting for a conventional bridge with Vo = 141.75V, $\alpha = 53.35^0$ calculated by comparison equations, are shown in Fig. 15.

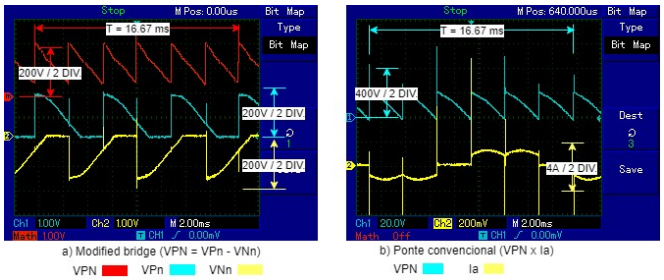

Fig. 15: VPN waveforms for the same average DC output voltage

The modified bridge waveforms for setting Vo = 118.77V, $\alpha = 70^0$, $\delta = 30^0$, are shown in Fig. 16.

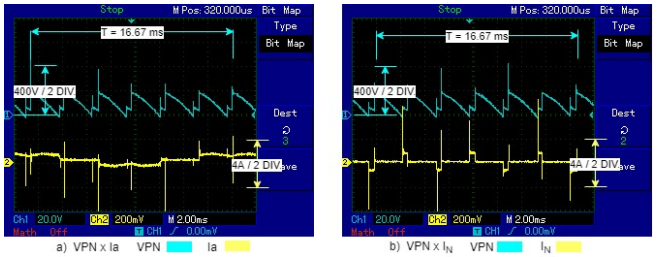

Fig. 16: Modified bridge – output voltage vs. input current

The waveforms for one setting for a modified bridge Vo = 118.77V, $\alpha = 70^0$, $\delta = 30^0$ and one setting for a conventional bridge with Vo = 118.77V, $\alpha = 57.01^0$ calculated by comparison equations, are shown in Fig. 17.

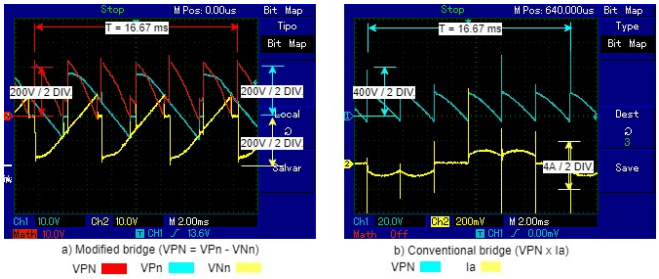

Fig. 17: VPN waveforms for the same average DC output voltage

4.4 Power factor and displacement factor for $0^0 \leq \alpha \leq 30^0$ and $\delta \geq 0^0$

The tests started with a first PQA (power quality analyzer) and the experimental values were consistent with theoretical concepts, but no closer with theoretical results. The tests were repeated with a second PQA and the experimental results were consistent with theoretical concepts and converged to the theoretical results.

The theoretical results and the experimental results for $0^0 \leq \alpha \leq 30^0$ and $\delta \geq 0^0$, for the test bench operating in mode 1 and in mode 2 with the same average DC output voltage, are shown in Table 3.

Table 3: Power factor and displacement factor ($0^0 \leq \alpha \leq 30^0$ e $\delta \geq 0^0$)

	Modified bridge					Conventional bridge		
Vo [4]	*α (⁰)*	*δ(⁰)*	*Cosφ1*	*I_1/I_{RMS}*	*PF*	*α(⁰)*	cosφ1	PF
	$0^{(1)}$	0	1.000	0.960	0.960	0.00	1.000	0.960
	$0^{(2)}$	0	0.998	0.953	0.955	0.00	0.997	0.955
297.10	$0^{(3)}$	0	1.000	0.955	0.955	0.00	1.000	0.955
	$0^{(1)}$	30	1.000	0.960	0.960	0.00	1.000	0.960
	$0^{(2)}$	30	0.998	0.953	0.955	0.00	0.997	0.955
297.10	$0^{(3)}$	30	1.000	0.955	0.955	0.00	1.000	0.955

Notes: [1] experimental results with the first PQA; [2] experimental results with the second PQA; [3] theoretical results obtained by equations; [4] the same DC average output voltage for modified and conventional bridges, obtained via equation (1) = equation (8).

4.5 Power factor and displacement factor for $30^0 < \alpha \leq 150^0$ and $\delta \geq 0^0$

The tests with the first PQA showed experimental values that were consistent with theoretical concepts, but no closer with

theoretical results. The tests were repeated with a second PQA and the experimental results were consistent with theoretical concepts and converged to the theoretical results.

The theoretical results and the experimental results for $30^0 < \alpha \leq 150^0$ and $\delta \geq 0^0$ for the test bench operating in mode 1 and mode 2 with the same average DC output voltage, are shown in Table 4.

Table 4: Power factor and displacement factor ($30^0 < \alpha \leq 150^0$ e $\delta \geq 0^0$)

	Modified bridge					Conventional bridge		
Vo[4]	α(⁰)	δ(⁰)	Cosφ1	I1/IRMS	PF	α(⁰)	Cosφ1	PF
	60(1)	0	0.780	0.897	0.700	47.10	0.687	0.650
	60(2)	0	0.697	0.901	0.628	52.45	0.616	0.582
171.53	60(3)	0	0.707	0.900	0.637	54.74	0.577	0.551
	60(1)	30	0.617	0.957	0.590	51.84	0.617	0.590
	60(2)	30	0.511	0.959	0.490	58.50	0.517	0.490
148.55	60(3)	30	0.500	0.955	0.477	60.00	0.500	0.477
	70(1)	0	0.730	0.877	0.640	53.35	0.603	0.570
141.75	70(3)	0	0.643	0.868	0.558	61.50	0.477	0.456
	70(1)	30	0.550	0.945	0.520	57.01	0.540	0.520
118.77	70(3)	30	0.423	0.943	0.399	66.44	0.400	0.382

Notes: (1) experimental results with the first PQA; (2) experimental results with the second PQA; (3) theoretical result obtained using the equations; (4) the same DC average output voltage for modified and conventional bridge, obtained, via equation (1) = equation (8).

4.6 AC harmonic distortion for $0^0 \leq \alpha \leq 30^0$ and $\delta \geq 0^0$

The PQA measured the individual and total AC current harmonic distortion and the harmonic spectrum. Neutral thyristors are ineffective for $0^0 \leq \alpha \leq 30^0$ and $\delta \geq 0^0$. Thus, AC harmonic are the same for test bench working as a modified and a conventional bridge. Neutral thyristors are ineffective for any δ value when considering the previous main angle interval.

The AC current harmonic spectrum for $\alpha = 0^0$ is shown in Fig. 18.

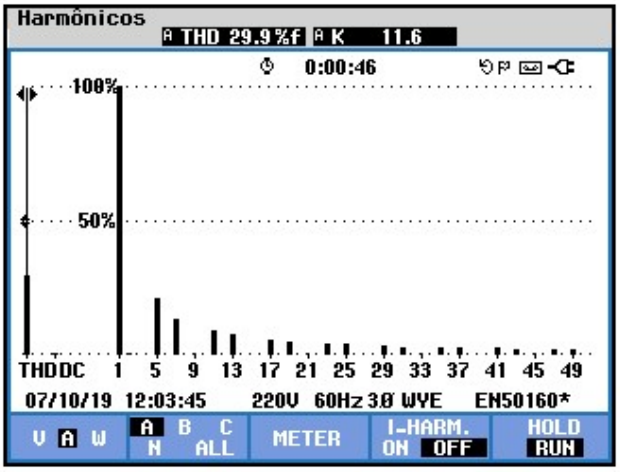

Fig. 18: Harmonic spectrum for modified and conventional bridge

The theoretical results and the experimental results for $0^0 \leq \alpha \leq 30^0$ and $\delta \geq 0^0$ for the test bench operating in mode 1 and mode 2 with the same average DC output voltage, are shown in Table 5.

Table 5: Current total harmonic distortion ($0^0 \leq \alpha \leq 30^0$ e $\delta \geq 0^0$)

	Modified bridge			Conventional bridge	
Vo [4]	α (⁰)	δ(⁰)	THD	α(⁰)	THD
	0(1)	0	29.9	0.00	29.9
	0(2)	0	30.0	0.00	30.0
297.10	0(3)	0	31.1	0.00	31.1
	0(1)	30	29.9	0.00	29.9
	0(2)	30	30.0	0.00	30.0
297.10	0(3)	30	31.1	0.00	31.1

Notes: (1) experimental results with the first PQA; (2) experimental results with the second PQA; (3) theoretical result obtained using the equations; (4) the same DC average output voltage for modified and conventional bridges, obtained via equation (1) = equation (8).

4.7 AC harmonic distortion for $30^0 < \alpha \leq 150^0$ and $\delta \geq 0^0$

The PQA measured the individual and total AC current harmonic distortion, and the harmonic spectrum for test bench operating in mode 1 with $30^0 < \alpha \leq 150^0$ and $\delta \geq 0^0$, and in mode 2 with $\alpha > 30^0$.

The AC current harmonic spectrum for a modified bridge with $\alpha = 60^0$ and $\delta = 0^0$, and a conventional bridge with $\alpha = 47.10^0$ is shown in Fig. 19.

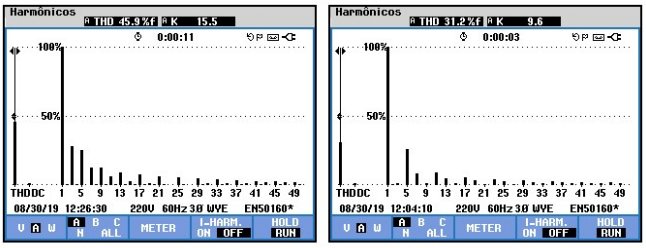

Fig. 19: Harmonic spectrum for modified and conventional bridge

The theoretical results and the experimental results for $30^0 < \alpha \leq 150^0$ and $\delta \geq 0^0$, for the test bench operating in mode 1 and mode 2 with the same average DC output voltage, are shown in Table 6.

Table 6: Current total harmonic distortion ($30^0 < \alpha \leq 150^0$ e $\delta \geq 0^0$)

	Modified bridge			Conventional bridge	
Vo [4]	α (⁰)	δ(⁰)	THD	α(⁰)	THD
	60(1)	0	45.9	47.10	31.2
	60(2)	0	48.1	52.45	34.7
171.53	60(3)	0	48.3	54.74	31.1
	60(1)	30	31.6	51.84	31.3
	60(2)	30	29.6	58.50	27.1
148.55	60(3)	30	31.1	60.00	31.1
	70(1)	0	54.0	53.35	32.0
141.75	70(3)	0	57.2	61.50	31.1
	70(1)	30	35.6	57.01	33.3
118.77	70(3)	30	35.2	66.44	31.1

Notes: (1) experimental results with the first PQA; (2) experimental results with the second PQA; (3) theoretical result obtained using

Table 6: Current total harmonic distortion ($30^0 < \alpha \leq 150^0$ e $\delta \geq 0^0$)

	Modified bridge			Conventional bridge	
Vo [4]	**α (^{0})**	**δ(^{0})**	**THD**	**α(^{0})**	**THD**
equations; [4] the same DC average output voltage for modified and conventional bridges, obtained via equation (1) = equation (8).					

5. MODIFIED BRIDGE IMPLEMENTATION AND COMPARARISON WITH A CONVENTIONAL BRIDGE

First a semi-controlled modified bridge was assembled, in which the neutral thyristors were replaced by diodes, similar to a modified bridge working with an AFCC set at $\delta = 0^0$, in order to evaluate some characteristics of the modified bridge, while the AFCC was in test. Subsequently, a test bench evaluated the proposed implementation.

The modified bridge operating between $0^0 \leq \alpha \leq 30^0$ and $\delta \geq 0^0$, showed identical results to a conventional bridge. The output voltage waveform depends on the main angle (α) and does not depend on the auxiliary angle (δ). The output voltage waveform is composed of two phase-to-phase input voltage in each phase input current half-cycle. The phase input current waveform depends on the main angle and does not depend on the auxiliary angle. There is no neutral input current waveform, regardless of the main angle and auxiliary angle. The AC current harmonic spectrum was identical. The total AC current harmonic distortion was identical. The power factor value was identical.

The modified bridge operating at $30^0 < \alpha \leq 150^0$ and $\delta \geq 0^0$, different results were found for the modified bridge and the conventional bridge. The output voltage waveform depends on the main angle (α) and the auxiliary angle (δ). The output voltage waveform is composed of two phase-to-phase input voltage and one phase-to-neutral input voltage in each half-cycle of the phase input current. The phase input current waveform depends on the main angle and auxiliary angle. The neutral input current waveform depends on the main angle and auxiliary angle. The current harmonic spectrum is different. There was higher AC current total harmonic distortion.

The phase thyristors work for a complete operating cycle of the modified bridge operation, slightly less than 120^0 due to the commutation interval. The neutral thyristors work for a complete operating cycle of the modified bridge operation, slightly less than 180^0 due to the commutation interval.

6. CONCLUSIONS

Bench tests were carried out to analyze and check theoretical values, and to fill gaps in comparative analysis for theoretical concepts versus experimental data. Based on the experimental results, we were able to conduct a comparative evaluation of modified and conventional bridges working according to their theoretical concepts.

The tests shows that the experimental data converges with theoretical concepts for the phase input current waveform, the neutral input current waveform, the DC output voltage waveform, and the operation as a conventional bridge and a modified bridge, for the theoretical main and auxiliary angles. The comparative analysis of the modified bridge versus the conventional bridge showed that there was convergence among experimental data and the theoretical concepts, since the power factor of the modified bridge was higher than the power factor of the conventional bridge, for the same average DC output voltage.

Other convergences for the modified bridge were observed, although they were not favorable for modified bridge when compared to a conventional bridge. There was greater total harmonic distortion of the AC current. The modified bridge is more expensive due to the two added neutral thyristors and an auxiliary firing control circuit. Lastly, the auxiliary firing control circuit is more complex, although we understand the auxiliary firing control circuit is an adaptation of the main firing control circuit.

We suggest that future studies analyze 12-pulse modified bridges with DC electric motors and 8 thyristor inverter bridges.

7. ACKNOWLEDGMENTS

The authors would like to thank Federal University of Itajubá allowing the author to conduct his research activities at the Electrical Energy System Institute from Federal University of Itajubá - ISEE UNIFEI.

8. REFERENCES

A.J.J. Rezek, V.F. Silva, L.E.B. Silva, J.P.G. Abreu, M.S. Miskulin (1990). Digital simulation of six and twelve-pulse converters with a modified thyristor bridge. IV Latin American Congress of Automatic Control. Puebla, Puebla, Mexico.

G.R.S. Mendonça (2002). Electronic circuit for the firing command of a three-phase thyristorised bridge (in Portuguese). End of Course Work, UNIFEI. Itajubá, MG, Brazil.

G. Olivier, V.R. Stefanovic (1980). Thyristor current source with an improved power factor. *Transactions on Industrial Electronics*, Vol. 1E-29, pp 299-307. IEEE.

J.A. Pomílio, (2019). Power electronic, Chapter 3 (in Portuguese).http://www.dsce.fee.unicamp.br/~antenor/pdffiles/eltpot/cap3.pdf.

J.M. Schaefer. Rectifier circuits: theory and design (1965). John Wiley and Sons, Inc. New York, USA.

M.C. Cardoso (2016/2017). Chopper transistor for driving card converter, using permanent magnet DC motor (in Portuguese). End of Course Work, UNIFEI. Itajubá, MG, Brazil.

M.L. Ramos, K.H.D.D. Carmo, R.B. Bicalho, R.D. Lorenzo, Â.J.J. Rezek (2017). 8 thyristor AC-DC modified converter bridge for power factor improvement (in Portuguese). SEPOC 2017 - 10º Seminar on Power Electronics and Control. Santa Maria, RS, Brazil.

V.R. Stefanovic. Power factor improvement with a modified phase-controlled converter (1979). *Transactions on Industry Applications*, Vol. IA-15, pp 193-201. IEEE.